Erschienen in: 37th European Photovoltaic Solar Energy Conference and Exhibition (EUPVSEC) : Proceedings. - München : WIP, 2020. - S. 414-417. - ISBN 3-936338-73-6

UPGRADE TECHNOLOGIES FOR SILICON PHOTOVOLTAICS – PART I: INDUSTRIAL SOLUTION TO MINIMIZE THE NEGATIVE IMPACT OF LIGHT INDUCED DEGRADATION

Thomas Pernau[1], Christian Derricks[2], Giso Hahn[2], Lailah Helmich[3, 4], Axel Herguth[2], Jan Schmidt[3, 4], Dominic Walter[3]
[1]centrotherm international AG, [2]Universitz of Konstanz, [3]Institute for Solar Energy Research Hamelin (ISFH),
[4]Institute of Solid State Physics, Leibniz University Hannover

ABSTRACT: This paper is to inform about Part I of a joint research project on optimum reduction of boron-oxygen related degradation and passivated contacts for PERC-based solar cells. It includes the application of investigated technologies into potential future cell designs such as PERT and bifacial solar cells. The joint project was merged from two individual project suggestions and therefore had two parts. This paper focuses on an industrial solution to minimize the negative impact of light induced degradation (LID) by:

- Investigating and understanding the nature of the degradation effect
- Applying the experimental results and concepts to industrially suppress LID
- Developing an optimized integrated firing-regeneration process for industrial application

The second part of this project is also covered in this conference [1]. The detailed project report (in German) has been published [2].
Keywords: LID, PERC, Rapid Thermal processing, Regeneration.

1 INTRODUCTION & OVERVIEW

Part one of the project concentrates on light induced degradation (LID) as described by Hashigami et al. [3]. The degradation conditions in all tests were limited to <100 mW/cm² light intensity at <40°C cell temperature. The level of understanding at the beginning of the project is summarized in [4]. There it is already suggested that a fast method can permanently deactivate recombination active boron-oxygen complexes in 30-40 s. This process can also be referred to as "regeneration" and especially "light induced regeneration" if light is used in the process [5, 6]. The industry partner in this project already had a regeneration belt furnace available. The project part I intention was to integrate the firing and regeneration process into one combined furnace. The typical parameter set for a regeneration furnace was elaborated, and the required firing process (including cooldown) for optimum regeneration was developed. With this knowledge, a shortened regeneration furnace was attached to a firing furnace with a revised, extremely compact cooling section. Towards the end of the project, a high intensity LED illumination device was introduced into the regenerator. The choice of illumination source was driven by optical safety rules and the physical properties explained in [7]. The regeneration was investigated with samples processed in an industrial regenerator and sister samples in accompanying lab experiments. Regeneration and degradation time constants have been determined for a number of materials. All regeneration experiments were confirmed by long-term LID tests of up to 1000 h. Stable lifetime / efficiency results can be expected after 48 h illuminated degradation test. Solar cells from standard production of various manufacturers were analyzed regarding the extent of BO-degradation and the ability to regenerate these solar cells. At the beginning of the project, for all surveyed manufacturers a significant degradation of η was observed during illuminated degradation test [8]. In all investigated cases, a regeneration process was able to restore the efficiencies as measured before degradation. During the project runtime, the model and understanding of regeneration has greatly improved. By the end of the project, a significantly deeper understanding of the involved boron-oxygen (BO) configurations has been established [9]. This can be confirmed by simulation studies within the project [12].

2 DETAILED WORK

The results are presented according to the work packages (WP) in the project.

2.1 Material evaluation and screening of commercially available solar cells (WP 2.1)

During the project time, 163 degradation experiments with 10 different wafer materials processed by 39 manufacturers have been tested. The relative average efficiency loss of unregenerated cells on p-type Cz material was > 3%, with extreme values > 6%. In 2015-2016, the regeneration process resulted in efficiency "improvements" so that regenerated cells reached a higher output as compared to as fired state (state A in the 3-state model, Fig. 5). This situation settled because it was most likely related to a not yet well established PERC cell process. By the end of the project and in own experiments with selected material, there was no more "improvement" by applying the regeneration process. Throughout the project, the long term stability of regenerated cells was better than 1% rel. efficiency loss during up to 1000 hours illumination. An extract from the manufacturer screening is shown in Fig. 1.

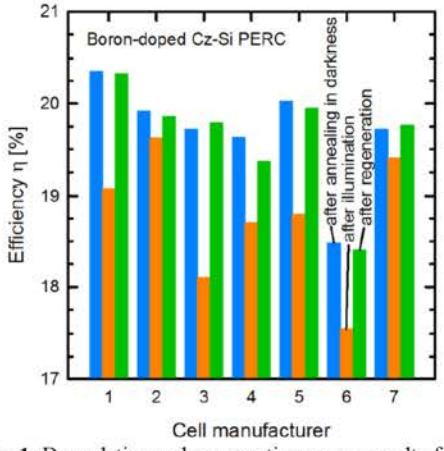

Fig. 1: Degradation and regeneration survey result of solar cells on 1 Ohm·cm Cz Si wafer material (from [10]).

2.2 Experiments on selected material (WP 2.2)

Selected material (wafer, cell precursors and solar cells) has been sourced from the free market for detailed investigation. Additionally, the company Solarworld provided wafers from their wafer production facility.

Fig. 2 shows an in-situ measurement of the cell current through a solar cell in darkness which resulted from applying a forward bias voltage of 520 mV. In parallel to the cell current, also the electroluminescence signal (EL Signal) was measured to determine the excess carrier density. From the change in Icell the rate constant can directly be determined.

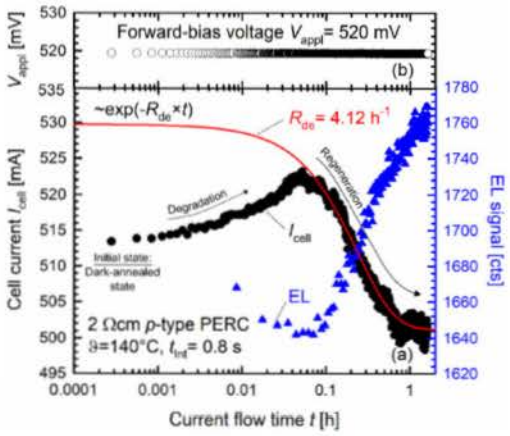

Fig. 2: In-situ measurement of the cell current through a solar cell in darkness by applying a forward bias voltage of 520 mV. In parallel to the cell current, also the electroluminescence signal (EL Signal) was measured to determine the excess carrier density. From the change in I_{cell} the rate constant can directly be determined (from [11]).

In our new developed setup to perform the regeneration in the absence of illumination, applying a constant forward bias V_{appl} voltage results in a rather constant Δn within the solar cell over the complete regeneration process. From the measured EL-Signal, shown in Fig. 2, the local junction voltage V_i was determined and then translated into the excess carrier concentration which is present under given regeneration conditions (T = 140°C, V_{appl} = 520 mV). By modifying the external voltage V_{appl}, the desired excess carrier density Δn in the current-driven degradation-regeneration experiment can be selected. This even allows selecting identical Δn regeneration conditions for different wafer materials. For two PERC cells made of different materials, the rate constant R_{de} depending on Δn is shown in Fig. 3. The result suggests a linear increase of R_{de} with Δn. For the first time, a functional correlation between Δn and R_{de} of the form $R_{de}[h^{-1}] = 0.66 \times 10^{-15}[cm^3h^{-1}] \times \Delta n[cm^{-3}]$ [11] was determined for a fixed temperature of 140°C.

In illuminated regeneration experiments with cells from various cell manufacturers, we determined the regeneration rate constants at 185°C and 1.5 suns equivalent illumination intensity. The result, plotted in Fig. 4, shows a broad range of R_{de} values, which could indicate different excess carrier densities within the cells under the same applied regeneration conditions.

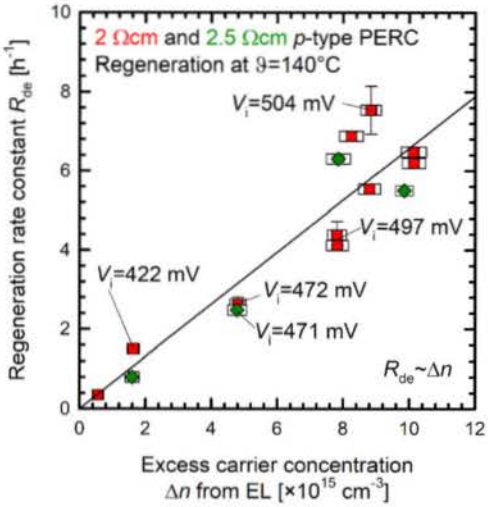

Fig. 3: Two "different" solar cells based on 2 Ohm·cm and on 2.5 Ohm·cm material are shown at varying injection levels imposed by the setting of the regeneration apparatus. The regeneration rate constant R_{de} shows a linear dependency on excess carrier concentration Δn, which was calculated from the calibrated EL signal. (From [11])

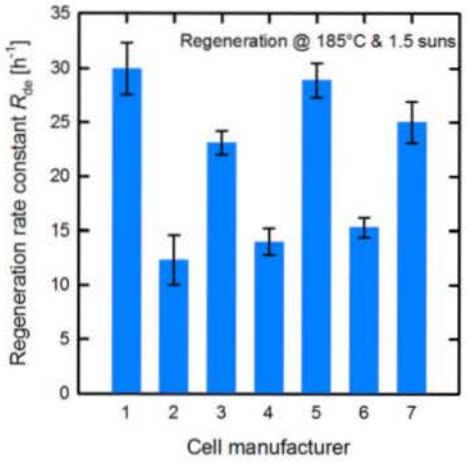

Fig. 4: Determination of the regeneration rate constant on selected material (commercially available solar cells in 2016). (From [10])

2.3 Refinement of the regeneration model (WP 3.1)

During the project runtime, the model refining for BO-correlated degradation and regeneration was supported with experiments. The understanding at the end of the project is published in [9]. For the considerations in this paper, we refer to the simplified model in Fig. 5.

The regeneration process in an illuminated belt furnace has been simulated using the simulation tool Cassandra [12]. For cross-checking with the real light intensity reached, a dedicated furnace intensity tracker has been developed [11]. The sample to be regenerated is in state A and then submitted to the regeneration process with up to 12 suns equivalent illumination (see explanation in [7]).

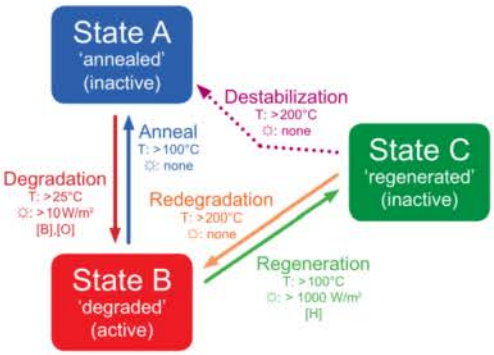

Fig. 5 3-state model (simplified regeneration model) from [9]

The aim of regeneration is to reach the highest possible population of state C. The illumination intensity also heats up the cell and overheating can destabilize recombination centers into state A. Two important regions of regeneration parameters have been identified:

- 6-10 suns illumination resulting in 250-300 °C cell temperature: state C can be fully reached within 10-15 s regeneration time, thermal depletion of state C is neglectable, the regeneration is stable
- > 10 suns illumination exceeding 300 °C sample temperature: state C can be thermally depleted into state A, the regeneration is incomplete.

For lab applications that tolerate a longer regeneration time, a sample illumination with 3-6 suns resulting in around 200°C sample temperature can be considered.

2.4 Industrial application of regeneration (WP 3.2)

Experiments and simulations in WP 3.1 (see previous section) suggest that an optimized regeneration furnace can be shortened to 10-15 s process time. Ideally, the cells are already pre-heated from the firing furnace. A shortened regenerator has been integrated into the fast firing furnace at the University of Konstanz. The regeneration takes place right after firing, before the cells cool down (Fig. 6). The optimum setting for the combined firing-regeneration process has been found in a parameter search experiment, the result is illustrated in Fig. 7.

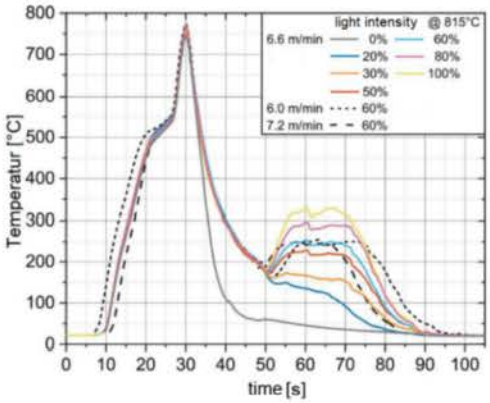

Fig. 6: Combined firing-regeneration process in an optimized firing-regeneration furnace. The furnace temperature has been recorded with a conventional temperature datalogger and thermocouples attached to the wafer surface. Illustration taken from [14].

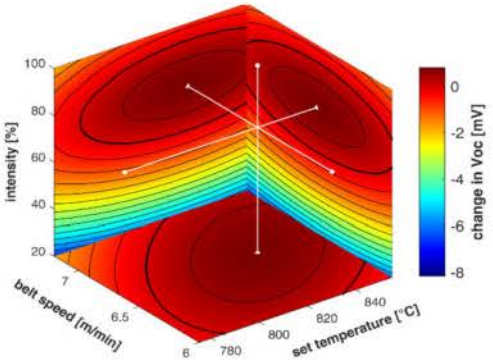

Fig. 7: Result of the parameter search experiment for the combined firing-regeneration furnace. For this experiment, the optimum result can be reached at a belt speed of 6.5 m/min, 820 °C set firing temperature and 80% regeneration light intensity (approx. 8 suns equivalent). Illustration taken from [13].

A parameter variation study with a wide spread of regeneration light intensity and time has been performed [14] to roughly cover the parameter range as compared to the simulation (see previous section). Regeneration stability has been deduced from V_{oc} loss of regenerated cells submitted to ≥ 48 h illuminated degradation. The result is illustrated in Fig. 8. Sufficient stability with the integrated furnace has been reached with approx. 6 suns equivalent irradiation. Cell temperatures > 300 °C are acceptable for a short time. Please note that the cell temperatures must be limited by water cooled sample support plates at the bottom of the furnace tunnel. The uncooled sample would overheat to > 400 °C.

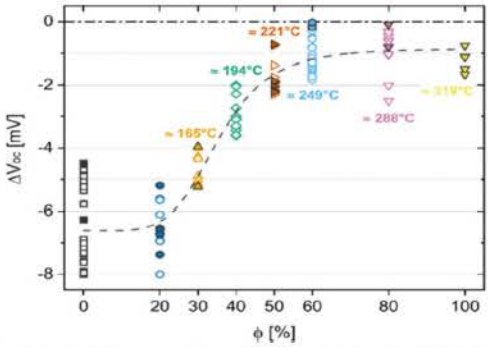

Fig. 8: Variation experiment for regenerator intensity and imposed heating effect from illumination. The lower the LID loss of the sample, the more complete is the regeneration result (deactivated BO-complexes in state C). Illustration taken from [14].

2.5 Long term stability tests (WP 4)

As it was initially not clear whether industrially regenerated cells are stable after only 10-30 seconds of regeneration, stability tests of regenerated cells have been performed. Figure 9 shows a stability test at room temperature and 0.1 suns light intensity for 45 cells regenerated in the industrial belt furnace (red boxes) and for two cells regenerated in a lab-type process (filled symbols). A virtually identical long-term behavior is observed after both processes with a significant gain of about 20 mV compared to the non-regenerated state B (after LID).

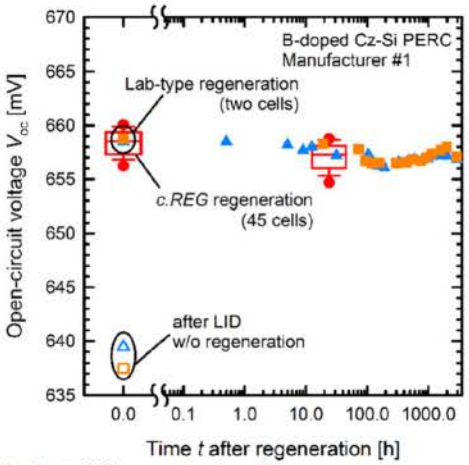

Fig. 9: Stability test of solar cells at room temperature and 0.1 suns light intensity after regeneration. The red boxes correspond to solar cells regenerated in the industrial belt furnace, whereas the filled symbols correspond to regenerated cells in a lab-type process. From [10].

Finally, to be sure that the regenerated cells do not suffer from module manufacturing, regenerated lifetime samples have been submitted to laminator temperature profiles for 10, 15 and 20 minutes. The stability has been tested for > 150 h to see any tong term effects. The result is illustrated in Fig. 10.

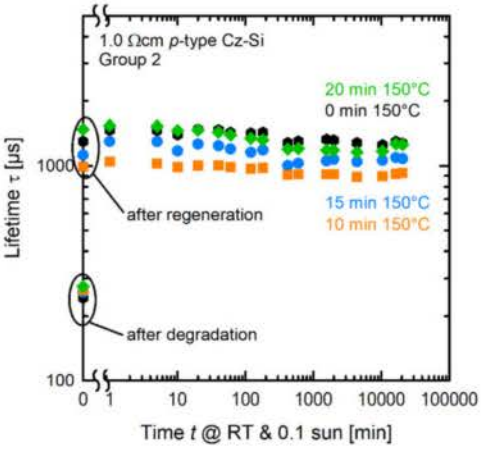

Fig. 10: Regenerated lifetime samples have been submitted to laminator temperature profiles followed by a long term light degradation test

3 CONCLUSION

The joint R&D project "Upgrade Technologies for Silicon Photovoltaics – Part I" has demonstrated the applicability of industrial regeneration of BO-complexes in a wide range of materials. An industrial regenerator can regenerate solar cells within a time range of 10-30 seconds. The regenerator can be made smaller and faster if it is combined with a firing furnace and an optimized parameter set is developed for the combination instrument. The regenerated cells are confirmed long term stable and do not suffer from thermal processing in module assembly.

4 ACKNOWLEDGEMENTS

This work was funded by the Federal Ministry for Economic Affairs and Energy under contract number 0325877. We would like to thank the colleagues of former SolarWorld Innovations GmbH for providing us with extraordinary material samples as long as possible.

5 REFERENCES

[1] F. Feldmann, B. Steinhauser, H. Nagel, T. Fellmeth, S. Mack, D. Ourinson, E. Lohmüller, J. Polzin, A. Moldovan, M. Bivour, F. Clement, J. Rentsch, M. Hermle, S.W. Glunz, T. Pernau; "Industrial TOPCon Solar Cells Realized by a PECVD Tube Process", this conference, 2AO.6.3

[2] A. Herguth, G. Hahn, D. Walter, L. Helmich, F. Feldmann, M. Hermle, S. Kreher, T. Schmidt, T. Pernau: „Upgrade Si-PV - Upgrade Technologien für die Silizium-Photovoltaik : Abschlussbericht zum Verbundprojekt : öffentlicher Teil, Zusammenfassung für alle Verbundpartner" https://doi.org/10.2314/KXP:1726190064

[3] H. Hashigami, y. Itakura, T. Saitoh, J. Appl. Phys. 93(7), 4240-4245 (2003).

[4] B. Hallam, P. Hamer, N. Nampalli, M. Abbott, M. Kim, D. Chen, A. Azmi, N. Gorman, H. Li, P.H.D. Lu, S. Wang, A. Ciesla, C. Chan, D. Payne, L. Mai, J. Ji, S.R. Wenham, Proc. 31th EUPVSEC, Hamburg 2015, p. 531-535, DOI: 10.4229/EUPVSEC20152015-2DO.16.4

[5] A. Herguth, G. Schubert, M. Kaes, G. Hahn, Proc. 4th WCPEC, Waikoloa 2006, p. 940-943

[6] X. Meng, Z. Xia, J. Wu, X.-S. Wang, G. Xing Proc. 31th EUPVSEC, Hamburg 2015, p. 470-472, DOI: 10.4229/EUPVSEC20152015-2DO.3.2

[7] A. Herguth, Energy Procedia 124, 53–59 (2017).

[8] T. Pernau, O. Romer, W. Scheiffele, A. Reichart, W. Jooss, Proc. 31st EUPVSEC2016, p. 918-920, DOI 10.4229/EUPVSEC20152015-2CV.4.3

[9] A. Herguth and B. Hallam, AIP Conf. Proc. 1999, 130006 (2018).

[10] D. Walter, L. Helmich, T. Pernau, O. Romer, J. Schmidt, Proc. 36th EUPVSEC, Marseille 2019, DOI: 10.4229/EUPVSEC20192019-2CV.2.101

[11] L. Helmich , D. Walter and J. Schmidt, IEEE Journal of Photovoltaics, vol. 9, no. 6, pp. 1472-1476, Nov. 2019

[12] A. Herguth and S. Wilking, "Cassandra – a tool for analysis and prediction of time resolved BO related defect dynamic on lifetime and cell level", Energy Procedia, Vol. 124 (2017), p. 60.

[13] A. Herguth, C. Derricks, G. Hahn, Proc. 36th EUPVSEC, Marseille 2019, p. 557-560, DOI 10.4229/EUPVSEC20192019-2CV.2.95

[14] C. Derricks, A. Herguth, G. Hahn, O. Romer, T. Pernau, Sol. Energ. Mat. Sol. Cells 195, 358-366 (2019).